Finite Element Method for Large-Amplitude Two-Dimensional Panel Flutter at Hypersonic Speeds

Carl E. Gray*
NASA Langley Research Center, Hampton, Virginia 23665
Chuh Mei†
Old Dominion University, Norfolk, Virginia 23529
and
C. P. Shore‡
NASA Langley Research Center, Hampton, Virginia 23665

A finite element approach is presented for determining the nonlinear flutter characteristics of two-dimensional panels using unsteady, third-order piston theory aerodynamics. Both nonlinear (large-amplitude) structural and nonlinear aerodynamic terms are considered in the finite element formulation. Solution procedures are presented to solve the nonlinear panel flutter and large-amplitude free vibration finite element equations. Nonlinear flutter analyses are performed for different boundary-support conditions and for various system parameters: plate thickness to length ratio h/a; Mach number M; flow-mass density to panel-mass density ratio; dynamic pressure λ; and maximum deflection to thickness ratio c/h. For large-amplitude free vibration, alternative classical analytical solutions are available for comparison. Linear aerodynamic and nonlinear structural finite element flutter results are compared with existing classical solutions, and nonlinear (aerodynamic and structure) results are compared among finite element findings presented in this study to assess the influence of including the nonlinearities associated with the third-order piston theory aerodynamics. In addition, the effect of varying the support conditions on the limit-cycle dynamic pressure is also evaluated.

Nomenclature

a	= panel length
a_e	= plate finite element length
a_1,a_2,a_3,a_4	= generalized out-of-plane coordinates
b_1,b_2,b_3,b_4	= generalized in-plane coordinates
c	= maximum panel deflection
D	= plate bending rigidity
e	= natural log base
h	= panel thickness
i	$= \sqrt{-1}$
M	= Mach number
$p,p_\infty,\mathbf{p}$	= aerodynamic pressure, freestream pressure, surface stress vector
q	= dynamic pressure
r	$= h/a$
u,w	= in-plane and out-of-plane panel deflections, respectively
V	= air velocity
$\{w\}$	= nondimensional element displacement
$\{W\}$	= nondimensional global finite element displacement
x,z	= coordinate axes
ϵ	= strain
Φ	= complex eigenvector
γ	= ratio of specific heats, $\gamma = 1.4$ for this investigation
ϕ	= out-of-plane interpolation functions
λ	$= 2qa^3/MD$
ρ,ρ_a	= plate and air mass densities, respectively
σ	= stress
τ	= nondimensional time
μ	$= \rho_a a/\rho h$
Ω	$= \alpha + i\omega$ complex eigenvalue
ν	= Poisson's ratio, $\nu = 0.3$
ξ	= nondimensional position coordinate
ω_0	$= \sqrt{D/\rho h a^3}$
ψ	= in-plane interpolation functions

Subscripts

cr	= critical
f	= flexural
l	= limit cycle
m	= membrane

Received Oct. 5, 1989; revision received Feb. 16, 1990.

*Aerospace Engineer, Facilities Engineering Division. Member AIAA.

†Professor, Department of Mechanical Engineering and Mechanics. Associate Fellow AIAA.

‡Aerospace Engineer, Structural Mechanics Division.

I. Introduction

PANEL flutter is the self-excited or self-sustained oscillation of an external panel of a flight vehicle when exposed to supersonic or hypersonic airflow. Panel flutter differs from wing flutter in that the aerodynamic forces resulting from the airflow act only on one side of the panel. In the context of small deflection (linear) structural theory, there is a critical value of the nondimensional dynamic pressure parameter λ_{cr} (or flow velocity) above which the panel motion becomes unstable and grows exponentially with time. Below this critical dynamic pressure, any disturbance to the panel results in motion that decays exponentially with time. A vast quantity of literature exists on linear panel flutter using different aerodynamic theories (e.g., Refs. 1–3 and many others). For panel flutter at high supersonic Mach numbers ($M > 1.7$), the aerodynamic theory applied for the most part is a quasisteady first-order piston theory aerodynamics.[4] Because of the resurgent interest in flight vehicles that will operate not only at high supersonic Mach numbers but well into the hypersonic regime, the proposed finite element approach employs unsteady nonlinear third-order piston theory aerodynamics. These aerodynamics, although several decades old, have been employed to

approximate the aerodynamic loads on the panel from local pressures generated by the body's motion as related to the local normal component of the fluid velocity; thus, a point-function relationship between the normal component of the fluid velocity and the local panel pressure is obtained. For high supersonic Mach numbers, these theories reasonably estimate the aerodynamic pressures.

In actuality, the panel not only bends but also stretches due to large-amplitude vibrations. Membrane tensile forces in the panel due to the induced stretching provide a limited stabilizing effect of the "hard-spring" type that restrains the panel motion to a bounded amplitude for limit-cycle oscillations with increasing amplitude as the dynamic pressure increases. The external skin of a flight vehicle thus can withstand velocities beyond the linear critical value λ_{cr}. McIntosh[5] investigated the effects of hypersonic nonlinear aerodynamic loadings on panel flutter. His findings, however, show that higher-order piston theory aerodynamics may, for some system parameters, produce a "soft-spring" effect that will predict lower flutter velocities than those predicted by first-order piston theory aerodynamics, although the effects of membrane tensile forces in the panel are included in the analysis. Two notable surveys on the subject of panel flutter for linear and nonlinear panel flutter are given by Dowell[6] and, most recently, by Reed et al.[7]

A number of classical analytical methods exist for the investigation of limit-cycle oscillations of panels in supersonic flow. However, because of the highly nonlinear nature of the aerodynamic theory, just a few researchers have investigated the limit-cycle oscillations of panels in hypersonic flow. McIntosh[5] integrated the nonlinear modal equations of motion for given initial conditions and observed the resultant panel motion vs time, until a limit-cycle response of constant amplitude independent of initial conditions was reached. Librescu[8] retained only the linear aerodynamic damping terms and derived the equations for an arbitrary number of modes using Galerkin's method. Typically, for the supersonic case, Galerkin's method is used in the spatial domain where the panel deflection is expressed in terms of one to six linear-normal modes. Various techniques in the temporal domain such as the time numerical integration,[9-11] harmonic balance,[12,13] and perturbation methods,[13,14] to cite a few, are employed. Also, nonlinear supersonic flutter of orthotropic panels was recently studied[15] using harmonic balance. All of the analytical investigations have been limited to two- or three-dimensional rectangular plates with all four edges simply supported or clamped. The classical approaches also show that, as a minimum, six linear-normal modes are required to achieve a converged solution for displacements and possibly more for stresses.[5,11]

Olson extended the finite element method to study the linear panel flutter problem.[16,17] Because of its versatile applicability, effects of aerodynamic damping, complex panel configurations, flow angularities, in-plane prestress, and laminated anisotropic panel properties can be included easily and conveniently in the finite element formulation. A review of linear panel flutter using finite element methods was given by Yang and Sung.[18]

Mei and Rogers applied the finite element method to study the supersonic limit-cycle oscillations of two-dimensional panels.[19,20] Rao and Rao[21] also investigated the large-amplitude supersonic flutter of two-dimensional panels with ends elastically restrained against rotation. Mei and Weidman,[22] Han and Yang,[23] and Mei and Wang[24] further extended the finite element method to treat supersonic limit-cycle oscillations of three-dimensional rectangular and triangular isotropic plates, respectively. Recently, Sarma, and Varadan[25] studied the nonlinear structural behavior of two-dimensional panels using the first-order piston theory aerodynamics. They presented two solution methods using a seventh-order displacement-based finite element. Their first method uses the nonlinear free-vibration mode shape as an approximation to the nonlinear panel flutter problem; alternately, their second method uses the linear panel-flutter mode shape as an initial estimate for an iterative solution process similar to those given in Refs. 18–24. Because of the resurgent interest in panel flutter at the high-supersonic/low-hypersonic speeds,[7] this paper extends the finite element method to investigate the limit-cycle oscillations of two-dimensional panels subject to hypersonic flow described by third-order piston theory aerodynamics.

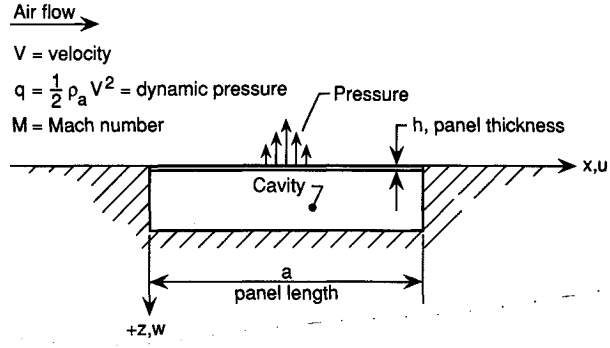

Fig. 1 Two-dimensional panel geometry.

Finite Element Formulation

Consider the two-dimensional flat panel of length a, thickness h, and mass density ρ, with air flowing above the panel at Mach number M shown in Fig. 1. It is assumed that the air flowing above the panel is in the positive x direction and that the effects of the cavity on the back side of the panel can be neglected. The sign convention to be followed is that positive flow is in the direction of increasing x and a positive deflection is into the cavity.

Hamilton's Principle for a Continuum

The general form of Hamilton's principle for a nonconservative elastic continuous medium is

$$\int_{t_1}^{t_2}\left[\int_V \rho \boldsymbol{u}_{,tt}\cdot\delta\boldsymbol{u}\,dV-\left(\int_V \boldsymbol{f}\cdot\delta\boldsymbol{u}\,dV+\int_S \boldsymbol{p}\cdot\delta\boldsymbol{u}\,dS-\int_V \sigma{:}\delta\epsilon\,dV\right)\right]dt=0 \tag{1}$$

The terms under the time integral represent the work done on the body at any time t by the resultant force in moving through the virtual displacement $\delta\boldsymbol{u}$; $\boldsymbol{f}$ is the body force, and is neglected in this formulation; $\boldsymbol{p}$ is the specified surface stress vector; and $\sigma{:}\delta\epsilon$ is a stress virtual-strain tensor product.

Constitutive and Strain-Displacement Relationships

For the two-dimensional isotropic plate, the stress-strain relationship becomes

$$\sigma=\frac{E}{(1-\nu^2)}\,\epsilon \tag{2}$$

The form of the strain-displacement relationship for an arbitrary point through the thickness h of the plate is as follows:

$$\epsilon = u_{,x}+\frac{1}{2}w_{,x}^{2}-z\,w_{,xx} \tag{3}$$

Aerodynamic Pressure Function

The virtual-work integral involving the surface stress vector is evaluated using the unsteady third-order piston theory aerodynamics[4,5] to develop the aerodynamic loads on the upper surface of the panel, which relates the local point function pressure generated by the panel's motion to the local normal component of the flow velocity. Thus, the aerodynamic pres-

sure loading as given by this theory is[5]

$$p - p_\infty = \frac{2q}{M}\left[\frac{1}{V}w_{,t} + w_{,x} + \frac{(\gamma+1)}{4}M \times \left(\frac{1}{V}w_{,t} + w_{,x}\right)^2 + \frac{(\gamma+1)}{12}M^2 w_{,x}^3\right] \quad (4)$$

The first two terms in the brackets in Eq. (4) constitute what is commonly referred to as the first-order piston theory aerodynamics, while Eq. (4) without the cubic term represents the second-order piston theory aerodynamics.

Element Representation

Using Eqs. (2–4) in Eq. (1) results in the following expression for Hamilton's principle for an element of length a_e:

$$\int_0^{a_e} \rho h\left(u_{,tt}\delta u + w_{,tt}\delta w\right)dx + \int_0^{a_e}\frac{2q}{M}\left[\frac{1}{V}w_{,t} + w_{,x} + \frac{(\gamma+1)}{4}M\left(\frac{1}{V}w_{,t} + w_{,x}\right)^2 + \frac{(\gamma+1)}{12}M^2 w_{,x}^3\right]\delta w\,dx + \int_0^{a_e}\frac{Eh}{(1-\nu^2)}\left[u_{,x}\delta u_{,x} + \frac{1}{2}w_{,x}^2\delta u_{,x} + u_{,x}w_{,x}\delta w_{,x} + \frac{1}{2}w_{,x}^3\delta w_{,x} + \frac{h^2}{12}w_{,xx}\delta w_{,xx}\right]dx = 0 \quad (5)$$

The displacement functions for the two-dimensional plate are chosen as

$$w(x,t) = [\phi_1(x)\ \phi_2(x)\ \phi_3(x)\ \phi_4(x)]\{w_f(t)\} \quad (6a)$$

$$u(x,t) = [\psi_1(x)\ \psi_2(x)\ \psi_3(x)\ \psi_4(x)]\{w_m(t)\} \quad (6b)$$

where $\{w_f\}$ and $\{w_m\}$ are the element nodal displacement quantities at the two ends of the plate:

$$\{w_f\} = \begin{Bmatrix} w_1 \\ \theta_1 \\ w_2 \\ \theta_2 \end{Bmatrix}, \qquad \{w_m\} = \begin{Bmatrix} u_1 \\ \epsilon_1 \\ u_2 \\ \epsilon_2 \end{Bmatrix} \quad (7)$$

The subscripts 1 and 2 refer to the two end nodes of the element and ϕ_j and ψ_j, $j = 1, \ldots, 4$, are the interpolation functions defined as

$$\phi_1 = \psi_1 = 1 - 3(x/a_e)^2 + 2(x/a_e)^3 \quad (8a)$$

$$\phi_2 = \psi_2 = x[1 - 2(x/a_e) + (x/a_e)^2] \quad (8b)$$

$$\phi_3 = \psi_3 = 3(x/a_e)^2 - 2(x/a_e)^3 \quad (8c)$$

$$\phi_4 = \psi_4 = x[(x/a_e)^2 - (x/a_e)] \quad (8d)$$

Using Eq. (6) in Eq. (5), dividing by a^3/D, letting $t = \tau/\omega_0$ and $x = a\xi$ (nondimensional time and position, respectively), $\lambda = 2qa^3/MD$ (nondimensional dynamic pressure), $\mu = \rho_a a/\rho h$ (nondimensional mass parameter), $r = h/a$, M = Mach number, and assuming constant properties over an element, the nondimensional element mass, stiffness, and aerodynamic influence matrices can be developed and written in terms of the interpolation functions and nodal quantities. Assembling the mass, stiffness, and aerodynamic influence matrices, the equations of motion for an element become

$$\begin{bmatrix}[m_f] & [0] \\ [0] & [m_m]\end{bmatrix}\begin{Bmatrix}\ddot{w}_f \\ \ddot{w}_m\end{Bmatrix} + \begin{bmatrix}([g]+[g_1]) & [0] \\ [0] & [0]\end{bmatrix}\begin{Bmatrix}\dot{w}_f \\ \dot{w}_m\end{Bmatrix} + \begin{bmatrix}([a]+[a_{f1}]+[a_{f2}]) & [0] \\ [0] & [0]\end{bmatrix}\begin{Bmatrix}w_f \\ w_m\end{Bmatrix} + \left(\begin{bmatrix}[k_{ff}] & [0] \\ [0] & [k_{mm}]\end{bmatrix} + \begin{bmatrix}[k_{1ff}] & [k_{1fm}] \\ [k_{1mf}] & [0]\end{bmatrix} + \begin{bmatrix}[k_{2ff}] & [0] \\ [0] & [0]\end{bmatrix}\right)\begin{Bmatrix}w_f \\ w_m\end{Bmatrix} = \{f\} \quad (9)$$

where $\{f\}$ is the internal element equilibrium forces, $[k]$ is the linear elastic stiffness matrix, and $[k_1]$ and $[k_2]$ are nonlinear stiffness matrices that depend linearly and quadratically upon displacements, respectively, and are defined as follows:

Mass:

$$[m_f] = \int_0^{a_e/a}\{\phi\}[\phi]\,d\xi \quad (10a)$$

$$[m_m] = \int_0^{a_e/a}\{\psi\}[\psi]\,d\xi \quad (10b)$$

Stiffness:

$$[k_{ff}] = \int_0^{a_e/a}\{\phi''\}[\phi'']\,d\xi \quad (10c)$$

$$[k_{mm}] = \frac{12}{r^2}\int_0^{a_e/a}\{\psi'\}[\psi']\,d\xi \quad (10d)$$

$$[k_{1mf}] = \frac{6}{r}\int_0^{a_e/a}\left(\frac{w_{,\xi}}{h}\right)\{\psi'\}[\phi']\,d\xi \quad (10e)$$

$$[k_{1fm}] = \frac{6}{r}\int_0^{a_e/a}\left(\frac{w_{,\xi}}{h}\right)\{\phi'\}[\psi']\,d\xi \quad (10f)$$

$$[k_{1ff}] = \frac{6}{r}\int_0^{a_e/a}\left(\frac{u_{,\xi}}{h}\right)\{\phi'\}[\phi']\,d\xi \quad (10g)$$

$$[k_{2ff}] = 6\int_0^{a_e/a}\left(\frac{w_{,\xi}}{h}\right)^2\{\phi'\}[\phi']\,d\xi \quad (10h)$$

Aerodynamic Influence:

$$[a] = \lambda\int_0^{a_e/a}\{\phi\}[\phi']\,d\xi \quad (10i)$$

$$[g] = \sqrt{\frac{\lambda\mu}{M}}\int_0^{a_e/a}\{\phi\}[\phi]\,d\xi \quad (10j)$$

$$[g_1] = \frac{1+\gamma}{4}\frac{\mu}{M}Mr\int_0^{a_e/a}\left(\frac{w_{,\tau}}{h}\right)\{\phi\}[\phi]\,d\xi \quad (10k)$$

$$[a_{f1}] = \frac{1+\gamma}{2} Mr \sqrt{\frac{\lambda\mu}{M}} \int_0^{a_e/a} \left(\frac{w_{,\tau}}{h}\right) \{\phi\}[\phi'] \, d\xi \tag{10l}$$

$$[a_{f1}] = \frac{1+\gamma}{4} \lambda \, Mr \int_0^{a_e/a} \left(\frac{w_{,\xi}}{h}\right) \{\phi\}[\phi'] \, d\xi \tag{10m}$$

$$[a_{f2}] = \frac{1+\gamma}{12} \lambda \, (Mr)^2 \int_0^{a_e/a} \left(\frac{w_{,\xi}}{h}\right)^2 \{\phi\}[\phi'] \, d\xi \tag{10n}$$

where

$$(\,)' = \frac{d(\,)}{d\xi}, \quad \dot{(\,)} = \frac{d(\,)}{d\tau}, \quad (\,)_{,\xi} = \frac{\partial(\,)}{\partial\xi}, \quad (\,)_{,\tau} = \frac{\partial(\,)}{\partial\tau}$$

The variational principle in Eq. (1) represents a finite element approach to study the limit-cycle oscillations of two-dimensional panels at hypersonic speeds. Unlike first-order piston theory aerodynamics that will produce two linear aerodynamic influence matrices ($[a]$ and $[g]$), the third-order piston theory aerodynamics yields, in addition to the same two linear matrices, four nonlinear aerodynamic influence matrices ($[g_1]$, $[a_{f1}]$, $[a_{f1}]$, and $[a_{f2}]$) where the aerodynamic matrices are functions of the system aerodynamic parameters, in particular the dynamic pressure λ. The aerodynamic influence matrices $[a]$ and $[g]$ are linear, whereas, $[g_1]$ and $[a_{f1}]$ depend linearly upon the time derivative of the displacements (generalized velocities). The other two matrices, $[a_{f1}]$ and $[a_{f2}]$, are linear and quadratic in the displacements. The symmetry in the first-order nonlinear stiffness matrix ($[k_{1mf}] = [k_{1fm}]^t$) has been preserved at the expense of transferring the nonlinearity on $w_{,\xi}$ to $u_{,\xi}$ by splitting $u_{,x}w_{,x}\delta w_{,x}$ in Eq. (5), thus producing the $[k_{1ff}]$ term.

System Finite Element Formulation and Solution Procedure

By assembling the finite elements for the entire system and applying the kinematic boundary conditions [e.g., for simply supports; $u(0) = u(a) = w(0) = w(a) = 0$], the equations of motion for the coupled (bending/membrane) system are of the form using the convention that upper case matrix notation pertains to assembled structure:

$$\begin{bmatrix} [M_f] & [0] \\ [0] & [M_m] \end{bmatrix} \{\ddot{W}\} + \begin{bmatrix} ([G] + [G_1]) & [0] \\ [0] & [0] \end{bmatrix} \{\dot{W}\}$$
$$+ \begin{bmatrix} ([A] + [A_{f1}] + [A_{f1}] + [A_{f2}]) & [0] \\ [0] & [0] \end{bmatrix} \{W\}$$
$$+ \left(\begin{bmatrix} [K_{ff}] & [0] \\ [0] & [K_{mm}] \end{bmatrix} + \begin{bmatrix} [K_{1ff}] & [K_{1fm}] \\ [K_{1mf}] & [0] \end{bmatrix} \right.$$
$$\left. + \begin{bmatrix} [K_{2ff}] & [0] \\ [0] & [0] \end{bmatrix} \right) \{W\} = \{0\} \tag{11}$$

where

$$\{W\} = \begin{Bmatrix} W_f \\ W_m \end{Bmatrix} \tag{12}$$

are the constrained nodal displacements of the assembled system. By neglecting the in-plane mass for the lower frequencies, Eq. (11) can be partitioned and written as two separate equations. Solving the partitioned equations for $\{W_m\}$ leads to the following reduced system equation in terms of the transverse displacement quantities $\{W_f\}$:

$$[M_f]\{\ddot{W}_f\} + [G + G_1]\{\dot{W}_f\} + ([K_{ff}] + [K_{1ff}]$$
$$- [K_{1fm}][K_{mm}]^{-1}[K_{1mf}] + [K_{2ff}])\{W_f\}$$
$$+ ([A] + [A_{f1}] + [A_{f1}] + [A_{f2}])\{W_f\} = \{0\} \tag{13}$$

where the relationship

$$\{W_m\} = -[K_{mm}]^{-1}[K_{1mf}]\{W_f\} \tag{14}$$

was used in deriving Eq. (13) by neglecting the in-plane mass $[M_m]$ in Eq. (11). This matrix equation, as written is a damped-vibration problem in the configuration space; and, as such, does not lend itself to standard eigenvalue solution algorithms. Thus, the approach to be adopted transforms the problem from the configuration space to a state space, which results in a more standard form of the eigenvalue problem. By making the transformation to the state space, the governing matrix equation Eq. (13) becomes

$$\begin{bmatrix} [M_f] & [0] \\ [0] & [I] \end{bmatrix} \begin{Bmatrix} \ddot{W}_f \\ \dot{W}_f \end{Bmatrix} + \begin{bmatrix} [D^*] & [K^*] \\ -[I] & [0] \end{bmatrix} \begin{Bmatrix} \dot{W}_f \\ W_f \end{Bmatrix} = \{0\} \tag{15}$$

where

$$[D^*] = [G] + [G_1] \tag{16a}$$

$$[K^*] = [K_{ff}] + [K_{1ff}] - [K_{1fm}][K_{mm}]^{-1}[K_{1mf}]$$
$$+ [K_{2ff}] + [A] + [A_{f1}] + [A_{f1}] + [A_{f2}] \tag{16b}$$

and $[I]$ is an identity matrix. The solution to the homogeneous problem is sought in the form of

$$\begin{Bmatrix} \dot{W}_f \\ W_f \end{Bmatrix} = \bar{c} \begin{Bmatrix} \Phi_1 \\ \Phi_2 \end{Bmatrix} e^{\Omega\tau} \tag{17}$$

where $\{\Phi_1\}$ and $\{\Phi_2\}$ are complex eigenvectors that are arranged as a single column vector, $\Omega = (\alpha + i\omega)$ is the complex eigenvalue, and $\bar{c}$ is a nonzero (scalar) constant displacement amplitude. Substituting the assumed response into Eq. (15) results in the following eigenvalue problem:

$$\bar{c}\left(\Omega \begin{bmatrix} [M_f] & [0] \\ [0] & [I] \end{bmatrix} + \begin{bmatrix} [D^*] & [K^*] \\ -[I] & [0] \end{bmatrix}\right) \begin{Bmatrix} \Phi_1 \\ \Phi_2 \end{Bmatrix} e^{\Omega\tau} = \{0\} \tag{18}$$

By expressing $e^{\Omega\tau}$ as a complex quantity in Euler form and requiring both coefficients of $\sin\omega t$ and $\cos\omega t$ to vanish, Eq. (18) can be written as two equations:

$$\bar{c}e^{\alpha\tau}\left(\Omega \begin{bmatrix} [M_f] & [0] \\ [0] & [I] \end{bmatrix} + \begin{bmatrix} [D^*] & [K^*] \\ -[I] & [0] \end{bmatrix}\right) \begin{Bmatrix} \Phi_1 \\ \Phi_2 \end{Bmatrix} \cos\omega\tau = \{0\} \tag{19}$$

$$i\bar{c}e^{\alpha\tau}\left(\Omega\begin{bmatrix}[M_f] & [0]\\ [0] & [I]\end{bmatrix}+\begin{bmatrix}[D^*] & [K^*]\\ -[I] & [0]\end{bmatrix}\right)\begin{Bmatrix}\Phi_1\\ \Phi_2\end{Bmatrix}\sin\omega\tau=\{0\} \tag{20}$$

Since $\bar{c}$ is nonzero, Eq. (11) is for a constrained system, and the solution sought is for all times greater than zero, both Eqs. (19) and (20) represent the same eigenvalue problem. To solve Eq. (19) or Eq. (20), the nonlinear matrices in Eqs. (16) need to be evaluated. Since all of the system quantities used in developing Eq. (15) are real, it must be concluded that the nodal response quantities must also be real.[3,20] As is generally the case with most nonlinear problems, numerous methodologies are available to obtain linearized solutions.[18-25] A significant focus of this study has been centered around linearizing the resulting nonlinear eigenvalue problem of Eq. (19) for synchronous motions. This can be accomplished by linearizing Eqs. (16) and employing an iterative solution procedure. Recalling Eq. (6a), the transverse nondimensional plate velocity and slope are

$$w_{,\tau}=[\phi]\{\dot{w}_f\} \tag{21a}$$

$$w_{,\xi}=[\phi']\{w_f\} \tag{21b}$$

Both of these quantities can be approximated from Eq. (17) by normalizing the eigenvector as follows and recognizing that $\{w_f\}$ is a real quantity and, as such, takes only the real part of the normalized Eq. (17):

$$\begin{Bmatrix}\dot{W}_f\\ W_f\end{Bmatrix}\simeq\frac{\bar{c}e^{\alpha\tau}}{|(\Phi_2)_k|}\begin{Bmatrix}|\Phi_1|\cos(\beta-\beta_k)\\ |\Phi_2|\cos(\beta-\beta_k)\end{Bmatrix}\cos\omega\tau \tag{22}$$

The quantity $|(\Phi_2)_k|$ is the magnitude of the largest displacement component of the eigenvector that corresponds to $\{W_f\}$, and β_k is the corresponding phase angle. Next, denote $c=\bar{c}e^{\alpha\tau}$ as the damped amplitude. Thus, it is clear from Eq. (22) that the sign of the real part of the eigenvalue controls the stability of the solution. The solution is stable for all α that are less than zero. For α equal to zero, then c equals $\bar{c}$ and the resulting solution corresponds to that of a limit-cycle oscillation. By letting

$$\begin{Bmatrix}\bar{\Phi}_1\\ \bar{\Phi}_2\end{Bmatrix}=\frac{1}{|(\Phi_2)_k|}\begin{Bmatrix}|\Phi_1|\cos(\beta-\beta_k)\\ |\Phi_2|\cos(\beta-\beta_k)\end{Bmatrix} \tag{23}$$

Eq. (22) becomes

$$\begin{Bmatrix}\dot{W}_f\\ W_f\end{Bmatrix}=c\begin{Bmatrix}\bar{\Phi}_1\\ \bar{\Phi}_2\end{Bmatrix}\cos\omega\tau \tag{24}$$

Using Eqs. (6) and (21), the (scalar magnitude) transverse nondimensional plate velocity and slope become

$$w_{,\tau}=c\,[\phi]\{\bar{\Phi}_1\}_j\cos\omega\tau \tag{25a}$$

$$w_{,\xi}=c\,[\phi']\{\bar{\Phi}_2\}_j\cos\omega\tau \tag{25b}$$

$$u_{,\xi}=c[\psi']\{(\bar{\Phi}_2)_m\}_j\cos\omega\tau \tag{25c}$$

In Eqs. (25), the column vectors $\{\bar{\Phi}_1\}_j$ and $\{\bar{\Phi}_2\}_j$ contain the appropriate global eigenvector quantities that correspond to the particular jth finite element and the column vector $\{(\bar{\Phi}_2)_m\}_j$ contains the appropriate membrane global eigenvectors using Eq. (14). Thus, with Eqs. (25), the nonlinear terms in Eq. (19) can be evaluated. By making use of the following identities

$$\cos\omega\tau=\left(\frac{1}{2}+\frac{1}{2}\cos 2\omega\tau\right)^{1/2} \tag{26a}$$

$$\cos^3\omega\tau=\frac{1}{4}(3\cos\omega\tau+\cos 3\omega\tau) \tag{26b}$$

and neglecting the higher harmonics, the following approximtions may be used to linearize Eq. (19):

$$\cos\omega\tau\simeq\sqrt{2}/2 \tag{27a}$$

$$\cos^3\omega\tau\simeq\frac{3}{4}\cos\omega\tau \tag{27b}$$

A similar approach may be used to linearize Eq. (20) and will result in the same linearized eigenvalue problem. Using Eq. (27a) in Eqs. (10) results in the following element matrices:

$$[k_{1fm}]=\frac{c}{h}[\bar{k}_{1fm}]\cos\omega\tau \tag{28a}$$

$$[k_{1mf}]=\frac{c}{h}[\bar{k}_{1mf}]\cos\omega\tau \tag{28b}$$

$$[k_{1ff}]=\left(\frac{c}{h}\right)^2[\bar{k}_{1ff}]\cos^2\omega\tau \tag{28c}$$

$$[k_{2ff}]=\left(\frac{c}{h}\right)^2[\bar{k}_{2ff}]\cos^2\omega\tau \tag{28d}$$

$$[g_1]=\frac{\sqrt{2}}{2}\left(\frac{c}{h}\right)[\bar{g}_1] \tag{28e}$$

$$[a_{t1}]=\frac{\sqrt{2}}{2}\left(\frac{c}{h}\right)[\bar{a}_{t1}] \tag{28f}$$

$$[a_{f1}]=\frac{\sqrt{2}}{2}\left(\frac{c}{h}\right)[\bar{a}_{f1}] \tag{28g}$$

$$[a_{f2}]=\left(\frac{c}{h}\right)^2[\bar{a}_{f2}]\cos^2\omega\tau \tag{28h}$$

where

$$[\bar{k}_{1fm}]=\frac{6}{r}\int_0^{a/a_e}([\phi']\{\bar{\Phi}_2\}_j)\{\phi'\}[\psi']\,d\xi \tag{29a}$$

$$[\bar{k}_{1mf}]=\frac{6}{r}\int_0^{a/a_e}([\phi']\{\bar{\Phi}_2\}_j)\{\psi'\}[\phi']\,d\xi \tag{29b}$$

$$[\bar{k}_{1ff}]=\frac{6}{r}\int_0^{a/a_e}([\psi']\{(\bar{\Phi}_2)_m\}_j)\{\phi'\}[\phi']\,d\xi \tag{29c}$$

$$[\bar{k}_{2ff}]=6\int_0^{a/a_e}([\phi']\{\bar{\Phi}_2\}_j)^2\{\phi'\}[\phi']\,d\xi \tag{29d}$$

$$[\bar{g}_1]=\frac{1+\gamma}{4}\frac{\mu}{M}Mr\int_0^{a/a_e}([\phi]\{\bar{\Phi}_1\}_j)\{\phi\}[\phi]\,d\xi \tag{29e}$$

$$[\bar{a}_{t1}]=\frac{1+\gamma}{2}Mr\sqrt{\frac{\lambda\mu}{M}}\int_0^{a/a_e}([\phi]\{\bar{\Phi}_1\}_j)\{\phi\}[\phi']\,d\xi \tag{29f}$$

$$[\bar{a}_{f1}]=\frac{1+\gamma}{4}\lambda\,Mr\int_0^{a/a_e}([\phi']\{\bar{\Phi}_2\}_j)\{\phi\}[\phi']\,d\xi \tag{29g}$$

$$[\bar{a}_{f2}]=\frac{1+\gamma}{12}\lambda\,(Mr)^2\int_0^{a/a_e}([\phi']\{\bar{\Phi}_2\}_j)^2\{\phi\}[\phi']\,d\xi \tag{29h}$$

define the linearized element matrices as represented in Eqs. (10). Assembling Eqs. (28) for the constrained system, condensing out the in-plane displacements according to Eq. (14), and using Eq. (27b) to linearize the remaining time functions

results in the following linearized eigenvalue problem:

$$\bar{c}e^{\alpha\tau}\left(\Omega\begin{bmatrix}[M_f] & [0]\\ [0] & [I]\end{bmatrix}+\begin{bmatrix}[\bar{D}] & [\bar{K}]\\ -[I] & [0]\end{bmatrix}\right)\begin{Bmatrix}\Phi_1\\ \Phi_2\end{Bmatrix}\cos\omega\tau=0 \tag{30}$$

where the linearized matrices $[\bar{D}]$ and $[\bar{K}]$ are defined as

$$[\bar{D}]=[G]+\frac{\sqrt{2}}{2}\left(\frac{c}{h}\right)[\bar{G}_1] \tag{31a}$$

$$[\bar{K}]=[K_{ff}]+\frac{3}{4}\left(\frac{c}{h}\right)^2[\bar{K}_{1ff}]-\frac{3}{4}\left(\frac{c}{h}\right)^2[\bar{K}_{1fm}][K_{mm}]^{-1}[\bar{K}_{1mf}]+\frac{3}{4}\left(\frac{c}{h}\right)^2[\bar{K}_{2ff}]+[A]+\frac{\sqrt{2}}{2}\left(\frac{c}{h}\right)[\bar{A}_{f1}]+\frac{\sqrt{2}}{2}\left(\frac{c}{h}\right)[\bar{A}_{f1}]+\frac{3}{4}\left(\frac{c}{h}\right)^2[\bar{A}_{f2}] \tag{31b}$$

The eigenvector is normalized so that the maximum value of the largest transverse displacement quantity in $\{W_f\}$ is unity with a reference phase angle of zero as given in Eq. (23). If Eq. (23) is normalized, then it can be scaled to a given limit-cycle amplitude c. Having normalized and scaled Eq. (24), u, w, and their derivatives for each element can be computed easily from Eqs. (25). Thus, the resulting estimate of the nodal quantities can be approximated from a previous solution of Eq. (30) as depicted in Fig. 2 by dropping the nonlinear terms in Eq. (30) and solving the linear eigenvalue problem. With the linear eigenvectors, the process just described can be used to approximate the quantities necessary to assemble the nonlinear element matrices in Eqs. (28); the same process is repeated until successive iterations yield the same eigenvalue, both real and imaginary, within acceptable limits,[20] and the same eigenvector, again within the limits of some convergence criteria.[20,26]

Therefore, for a given panel configuration and dynamic pressure, the system eigenvalues and eigenvectors can be computed. As the dynamic pressure is increased monotonically from zero ($\lambda=0$ corresponds to in vacuo large-amplitude free vibration), the symmetric real-and-positive-definite stiffness matrix is perturbed by the skewed ($[A]$, $[\bar{A}_{f1}]$, $[\bar{A}_{f1}]$, and $[\bar{A}_{f2}]$) and symmetric ($[G]$ and $[\bar{G}_1]$) aerodynamic influence matrices so that two of the eigenvalues approach each other until they coalesce. A critical dynamic pressure λ_{cr} for the linear structure ($c/h=0$) and a limit-cycle dynamic pressure λ_l for the nonlinear structure are determined when the real part of the eigenvalue approaches positive values for a fixed dynamic pressure (see Fig. 4 for example).

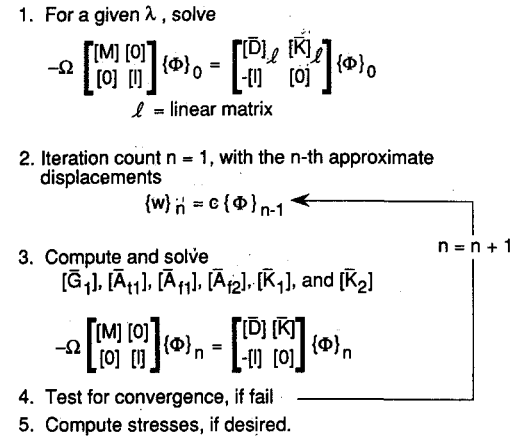

Fig. 2 Nonlinear panel flutter solution procedure.

Results and Discussion

A study to determine the number of finite elements necessary to achieve a converged solution was performed. It was found that there was approximately 2% difference between an eight-element solution and a twelve-element solution, whereas there was less than 0.1% difference between twelve- and sixteen-element solutions. Therefore, all of the results presented in this study are for twelve-element solutions.

Large Amplitude In Vacuo Vibration

A comparison between various classical analytical solutions and a twelve-element solution was performed for simply supported and clamped panels. The first comparison is for a simply supported panel. Analytical solutions using two different approaches from Ref. 27 and Woinowsky-Kreiger's elliptic-function results[28] are also shown in Table 1. All of these methods, assumed time mode,[27] the Galerkin approach,[27] and elliptic-function, used a single linear mode to separate the spatial and time dependence on the displacements in the governing equations. The finite element method also uses a single mode, but it is a nonlinear updated mode that is iterated in Eq. (30) until subsequent iterations produce the same mode shape and eigenvalue. The comparison between the single-mode elliptic-function solutions and the finite element method is favorable for both modes.

The second comparison is with Yamaki and Mori's three-mode Galerkin procedure[29] for the large-amplitude vibration

Table 1 Comparison of large-amplitude free vibration $(\omega/\omega_0)_n$ for a simply-supported panel

Amplitude c/h	Mode n	12 finite elements	Woinowsky-Kreiger[28] elliptic function	Assumed time mode[27]	Ritz-Galerkin[27]
0.0	1	1.0000	1.0000	1.0000	1.0000
	2	1.0000	1.0000		
0.2	1	1.0436	1.0439	1.0296	1.0440
	2	1.0441	1.0439		
0.4	1	1.1662	1.1644	1.1136	1.1662
	2	1.1662	1.1644		
0.6	1	1.3455	1.3397	1.2410	1.3454
	2	1.3452	1.3397		
0.8	1	1.5623	1.5506	1.4000	1.5620
	2	1.5621	1.5506		
1.0	1	1.8024	1.7844	1.5811	1.8028
	2	1.8027	1.7844		
1.2	1	2.0588	2.0335	1.7776	2.0591
	2	2.0590	2.0335		

Table 2 Comparison of large-amplitude vibration of a clamped beam

	Nondimensional frequency	
Amplitude c/h	Theory-Galerkin assumed space mode Yamaki and Mori[29]	Finite element method
0.0665	22.4	22.40
0.5307	24.0	24.00
0.9833	27.5	27.53
1.4571	32.5	32.55
2.0451	40.0	39.81
2.6602	50.0	48.06
3.0683	60.0	53.73

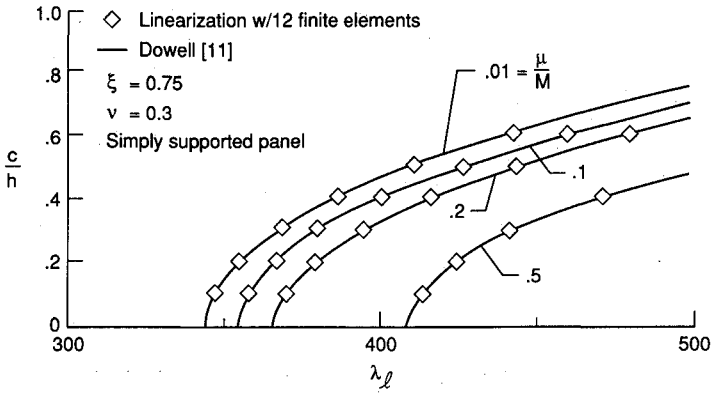

Fig. 3 Comparison of limit-cycle flutter amplitude ratios with Dowell's solution for a simply-supported panel.

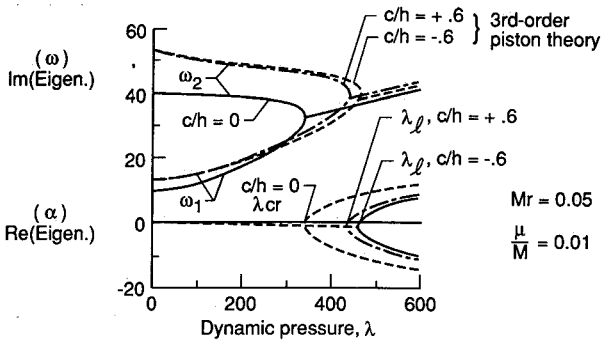

Fig. 4 Eigenvalue variation with nondimensional dynamic pressure parameter for a simply-supported panel. ($Mr = .05$ and $\mu/M = .01$)

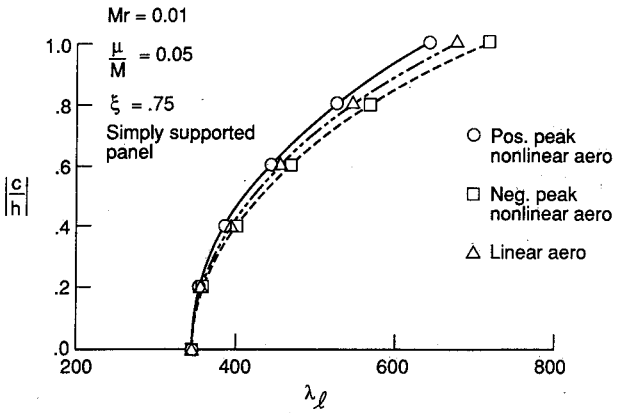

Fig. 5 Comparison of first- and third-order piston theory aerodynamics on large-amplitude panel flutter (panel deflection at $x/a = .75$).

of a clamped beam. The nondimensional first-mode frequency for several amplitude ratios is presented in Table 2. These results compare well for c/h ratios up to approximately two. For amplitude ratios greater than two, the finite element results exhibit a "softer" response. Thus, using the procedure as described earlier yields finite element results that correlate well with established classical methods. This procedure can best be described as a linearized updated mode with a nonlinear time function approximation (LUM/NTF) method.

Nonlinear Structure and Linear Aerodynamics

A comparison was made with Dowell's six-mode limit-cycle oscillation results[11] using first-order piston theory aerodynamics. However, since the finite element formulation presented here differs slightly from the formulation presented in Ref. 11, the finite element in-plane stiffness matrices were scaled by $(1-\nu^2)$ to correlate with Eq. (1.4) of Ref. 11. This comparison is shown in Fig. 3 for several μ/M ratios. The finite element results, using the LUM/NTF linearizing method, agree extremely well with Dowell's results.[11]

Simply Supported Panel and Effects of System Parameters

The effects of the nonlinear structure and hypersonic third-order piston theory aerodynamics (for $c/h = \pm 0.6$), when compared to the linear structure and first-order piston theory aerodynamics ($c/h = 0$) for a simply supported panel, can be seen in Fig. 4, which depicts coalescence of the first and second linear modes at $\lambda = 343.35$. Classical analytical methods establish coalescence at $\lambda = 343.35$. Thus, linear finite element results compare well with linear classical solutions. The complete panel behavior is characterized by plotting the complex eigenvalue $(\alpha + i\omega)$ variation with increasing dynamic pressure λ. These variations are shown in Fig. 4 for the first two modes. As λ increases from zero (in vacuo), the $\mathrm{Im}(\Omega_1) = \omega_1$ for the first mode increases and the $\mathrm{Im}(\Omega_2) = \omega_2$ for the second mode decreases until the two modes coalesce. When damping is present, the instability sets in at a somewhat higher value of λ as indicated when $\alpha = 0$. This point (λ_{cr}) for the linear cases is a function of the system parameter μ/M [see Eq. (10)]; however, for the nonlinear case λ_l is a function of μ/M and Mr. Other than the obvious increase in λ at coalescence, the nonlinear aerodynamics also produces another significant effect which is seen by the dependence of λ on the sign of the assumed mode shape. McIntosh[5] attributes this effect to the nonlinear $w_{,x}^2$ term in Eq. (4) that produces an overpressure which in turn tends to push the panel into the cavity.

A comparison between the first-order and third-order piston theory aerodynamics is shown in Fig. 5. Again, the effect of the sign of the mode shape on the response is noted. The first-order piston theory aerodynamics and nonlinear structural theory show no response change relative to the sign of the assumed mode; in fact, the first-order response for these particular system parameters falls between the $\pm c/h$ results for the third-order theory. Thus, for the $+c/h$ amplitude ratios, the effect of including the third-order theory aerodynamics is destabilizing when compared to the first-order theory, and stabilizing for $-c/h$ amplitude ratios. As cited in Ref. 5 and noted in Fig. 4, the change in the frequency oscillation is quite small. This resulted in the panel deflection shapes at λ_l for both the first- and third-order piston theory aerodynamics being very similar—the maximum deflection occurred at $x/a = 0.75$.

Since λ_l depends on the system parameters μ/M and Mr, the effect of increasing these parameters for a variation in λ results in a change in peak displacement, as shown in Fig. 6.

For the parameters noted on the figure and a limit-cycle amplitude less than one-half of a plate thickness, the amplitude-dynamic pressure relationship can be reasonably estimated by first-order piston theory aerodynamics. Because of the strong influence of the nonlinear effects from both the geometry ("hardening") and the aerodynamics ("softening"), these results suggest that third-order piston theory aerody-

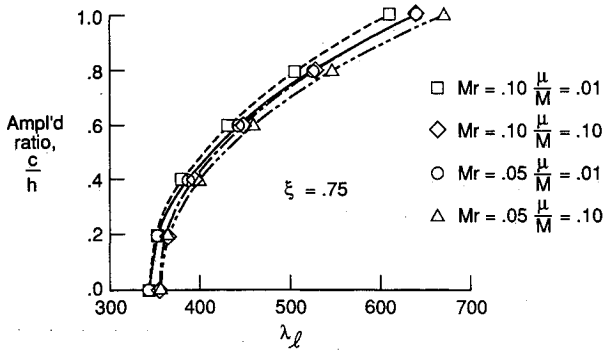

Fig. 6 Effects of aerodynamic and geometry parameters on limit-cycle flutter amplitude at $x/a = .75$ for simply-supported panels.

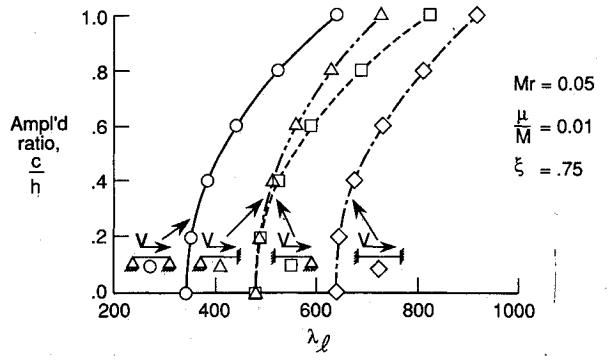

Fig. 7 Effects of support conditioning on limit-cycle flutter amplitude at $x/a = .75$. ($Mr = .05$ and $\mu/M = .01$)

namics should be employed for limit-cycle amplitudes that are greater than one-half of a plate thickness.

Boundary Support Effects

In Fig. 7, the nondimensional panel amplitude of the limit-cycle oscillation is given as a function of λ_l for various edge restraints. The most interesting result is that the limit-cycle motions are different for hinged-clamped and clamped-hinged panels. This occurs because the constrained system matrices are different for these support conditions. This condition is difficult to evaluate analytically; however, it is easy to account for when using finite elements. It is also interesting to note that the slopes for the various boundary conditions behave according to the trailing-edge support condition.

Nonlinear Aerodynamic Effects

Another interesting aspect is the influence the aerodynamic nonlinear terms have on the motion of the panel as it oscillates at a high dynamic pressure. Table 3 summarizes, for the parameters shown, a comparison between the first-, second-, and third-order piston theory aerodynamics and the effect of neglecting each of the nonlinear aerodynamic terms independently. The term that has the most significant influence when deleted is the $w_{,x}^2$.

It should be pointed out that nondimensional parameters may be grouped in two ways. For example, Refs. 3 and 5 each elect to nondimensionalize the $w_{,t}$ term differently. Reference 5 chooses to make the coefficient a function of λ, whereas Ref. 3 eliminates λ in favor of a nondimensional damping parameter. The work presented here follows the parameter notation of Ref. 5 so that the in vacuo free vibration of a panel can be assessed by setting $\lambda = 0$.

Concluding Remarks

An analytical procedure for large-amplitude panel flutter at hypersonic speeds has been developed using the finite element method. Extension of the finite element panel flutter formulation to include nonlinear hypersonic aerodynamic loading (third-order piston theory aerodynamics) is presented. A method of linearizing the assumed limit-cycle time function has been presented. The LUM/NTF method consists of using a linearized updated mode with a nonlinear time-function approximation and gives results that compare extremely well with classical analytical results for in vacuo large-amplitude vibration and large-amplitude panel flutter using linear aerodynamics. Results illustrate the influence of various combinations of support conditions on the limit-cycle amplitude vs dynamic pressure relations. Results also show the destabilizing effect of the unsteady third-order piston theory aerodynamics compared to the quasisteady first-order piston theory aerodynamics theory that is usually employed.

References

[1]Laurenson, R. M., and McPherson, J. I., "Design Procedures for Flutter-Free Surface Panels," NASA CR-2801, 1977.

[2]Cunningham, H. J., "Flutter Analysis of Flat Rectangular Panels Based on Three-Dimensional Supersonic Unsteady Potential Flow," NASA TR R-256, 1967.

[3]Dugundji, J., "Theoretical Considerations of Panel Flutter at High Supersonic Mach Numbers," *AIAA Journal,* Vol. 4, July 1966, pp. 1257-1266.

[4]Ashley, H., and Zartarian, G., "Piston Theory—A New Aerodynamic Tool for the Aeroelastician," *Journal of the Aeronautical Sciences,* Vol. 23, Dec. 1956, pp. 1109-1118.

[5]McIntosh, S. G., Jr., "Theoretical Considerations of Some Nonlinear Aspects of Hypersonic Panel Flutter," Final Rept., Sept. 1, 1965 to Aug. 31, 1970, NASA Grant NGR 05-020-102, Dept. of Aeronautics and Astronautics, Stanford Univ., Stanford, CA, Nov. 1974.

[6]Dowell, E. H., "Panel Flutter: A Review of the Aeroelastic Stability of Plates and Shells," *AIAA Journal,* Vol. 8, March 1970, pp. 385-399.

[7]Reed, W. H., Hanson, P. W., and Alford, W. J. "Assessment of Flutter Model Testing Relating to the National Aerospace Plane," NASP CR-1002, 1987.

[8]Librescu, L., "Aeroelastic Stability of Orthotropic Heterogeneous Thin Panels in the Vicinity of the Flutter Critical Boundary," *Journal de Mechanique,* Vol. 4, March 1965, pp. 51-76.

[9]Ventres, C. S., and Dowell, E. H., "Comparison of Theory and Experiment for Nonlinear Flutter of Loaded Plates," *AIAA Journal,* Vol. 8, Nov. 1970, pp. 2022-2030.

[10]Dowell, E. H., "Nonlinear Oscillations of a Fluttering Plate II," *AIAA Journal,* Vol. 5, Oct. 1967, pp. 1856-1862.

[11]Dowell, E. H., "Nonlinear Oscillations of a Fluttering Plate," *AIAA Journal,* Vol. 4, July 1966, 1267-1275.

[12]Eastep, F. E., and McIntosh, S. C., "Analysis of Nonlinear Panel Flutter and Response under Random Excitation or Nonlinear Aerodynamic Loading," *AIAA Journal,* Vol. 9, March 1971, pp. 411-418.

Table 3 Effects on λ_l by neglecting higher-order terms in piston theory aerodynamics [Eq. (4)][a]

Amplitude c/h	First-order piston theory	Second-order piston theory	Third-order piston theory	Neglect $w_{,x}^3$	Neglect $w_{,x}^2$	Neglect $w_{,t}^2$	Neglect $w_{,t}w_x$
0.0	355.09	355.09	355.09	355.09	355.09	355.09	355.09
0.2	367.44	364.68	364.61	364.68	367.60	364.61	364.53
0.4	405.19	398.89	398.72	398.89	405.32	398.73	398.42
0.6	470.38	458.74	458.27	458.74	470.37	458.29	457.74
0.8	568.20	547.87	546.96	547.87	568.07	547.03	545.97
1.0	708.88	673.51	672.01	673.51	708.86	672.03	670.51

[a]Simply supported panel, $Mr = 0.05$ and $\mu/M = 0.1$.

[13]Kuo, C. C., Morino, L., and Dungundji, J., "Perturbation and Harmonic Balance Methods for Nonlinear Panel Flutter," *AIAA Journal,* Vol. 10, Nov. 1972, pp. 1479–1484.

[14]Morino, L., "A Perturbation Method for Treating Nonlinear Panel Flutter Problems," *AIAA Journal,* Vol. 7, March 1969, pp. 405–410.

[15]Eslami, H., "Nonlinear Flutter and Forced Oscillations of Rectangular Symmetric Cross-Ply and Orthotropic Panels Using Harmonic Balance and Perturbation Method," Ph.D. Dissertation, Old Dominion Univ., Norfolk, VA, 1987.

[16]Olson, M. D., "Finite Elements Applied to Panel Flutter," *AIAA Journal,* Vol. 5, Dec. 1967, pp. 2267–2270.

[17]Olson, M. D., "Some Flutter Solutions Using Finite Elements," *AIAA Journal,* Vol. 8, April 1970, 747–752.

[18]Yang, T. Y., and Sung, S. H., "Finite-Element Panel Flutter in Three-Dimensional Supersonic Unsteady Potential Flow," *AIAA Journal,* Vol. 15, Dec. 1977, pp. 1677–1683.

[19]Mei, C., and Rogers, J. L., Jr., "Application of NASTRAN to Large-Deflection Supersonic Flutter of Panels," NASA TM X-3428, Oct. 1976, pp. 67–97.

[20]Mei, C., "A Finite-Element Approach for Nonlinear Panel Flutter," *AIAA Journal,* Vol. 15, Aug. 1977, pp. 1107–1110.

[21]Rao, K. S., and Rao, G. V., "Large-Amplitude Supersonic Flutter of Panels with Ends Elastically Restrained Against Rotation," *Computers and Structures,*" Vol. 11, March 1980, pp. 197–201.

[22]Mei, C., and Weidman, D. J., "Nonlinear Panel Flutter—A Finite-Element Approach," *Computational Methods for Fluid-Structure Interaction Problems,* AMD-Vol. 26, edited by Belytscnke, T., and Geers, T. L., American Society of Mechanical Engineers, Atlanta, GA, Nov. 1977, pp. 139–165.

[23]Han, A. D., and Yang, T. Y., "Nonlinear Panel Flutter Using High-Order Triangular Finite Elements," *AIAA Journal,* Vol. 21, Oct. 1983, pp. 1453–1461.

[24]Mei, C., and Wang, H. C., "Finite-Element Analysis of Large-Amplitude Supersonic Flutter of Panels," *Proceedings International Conference on Finite-Element Methods,* Shanghai, China, Gordon and Breach Science Publishers, Inc., 1982, pp. 944–951.

[25]Sarama, B. S., and Varadan, T. K., "Nonlinear Panel Flutter by Finite-Element Method," *AIAA Journal,* Vol. 26, May 1988, pp. 566–574.

[26]Bergan, P. G., and Clough, R. W., "Convergence Criteria for Iterative Processes," *AIAA Journal,* Vol. 10, Aug. 1972, pp. 1107–1108.

[27]Ray, J. D., and Bert, C. W., "Nonlinear Vibrations of Beams with Pinned Ends," Transactions of the American Society of Mechanical Engineers, *Journal of Engineering for Industry,* Vol. 91, Nov. 1969, pp. 997–1044.

[28]Woinowsky-Krieger, S., "The Effects of Axial Force on the Vibration of Hinged Bars," *Journal of Applied Mechanics,* Vol. 17, March 1950, pp. 35–36.

[29]Yamaki, N., and Mori, A., "Nonlinear Vibrations of a Clamped Beam with Initial Deflection and Initial Axial Displacement, Pt. I: Theory," *Journal of Sound and Vibration,* Vol. 71, Aug. 1980, pp. 333–346.